Electrical Analogue Model of an Integrated Circulator

J. R. Maddocks, P. Maddocks, A. Kashani

Atlas Scientific
San Jose, CA 95120

ABSTRACT

The problem of cooling gimbaled optics and LWIR focal planes can be solved by placing the entire cryocooler on the gimbal. However, a large mass penalty is paid for such configurations, because the gimbal itself must grow in size and mass in order to support the cryocooler[1]. To address the requirements of cooling across a two-axis gimbal, flexible joint, or to multiple locations on a spacecraft, we are developing an Integrated Circulator – a lightweight, continuous-flow cooling loop directly integrated into the coldhead of a Pulse Tube Cryocooler (PTC). The basis of the Integrated Circulator is a cold rectifier that converts the oscillating flow of the PTC into a steady flow of cold gas that can readily be distributed over distances of several meters to multiple loads. Because the cooling loop can be made of capillary tubing, it is easily made mechanically compliant by means of coiling, thus allowing the cryocooler to be located off gimbal. In this paper, we describe an electrical analogue model of the cooling loop and use it to investigate the dependence of average mass flow rate on buffer volume size. The calculations agree well with recent measurements.

INTRODUCTION

In future space applications, thermal loads will be cooled by small, centrally-located, closed-cycle cryocoolers. The coolers that offer the greatest potential for such applications are regenerative systems such as the Pulse Tube Cooler (PTC) and Stirling cooler. Conductive cooling across gimbaled or flexible joints or of multiple distributed or broad area thermal loads is not a viable option, because of the need for massive copper straps. Instead, a cooling loop coupled to the cryocooler coldhead via a heat exchanger will be required for these applications. The most commonly suggested options for such a cooling loop are the Loop Heat Pipe (LHP)[2] or its close cousin the Capillary Pumped Loop (CPL) and the mechanically driven Pumped Fluid Loop (PFL) with either a cryogenic pump[3] or ambient pump[4]. These options each require a separate pump and cooling loop dedicated to circulating cold fluid through a heat exchanger thermally connected to the coldhead of a cryocooler.

As an alternative, we are developing an Integrated Circulator (IC) for such applications. The IC has a rectifier at the cold heat exchanger that converts the oscillating flow of a Pulse Tube or Stirling cooler into a steady flow of cold, supercritical gas. Thermal integration of a fluid loop with the cooler is a given as the fluid is obtained from and returns to the gas volume of the cooler. This approach has advantages over competing technologies in that it eliminates the independent circulating pump – its mass, its potential reliability problems and its parasitic power

Cryocoolers 17, edited by S.D. Miller and R.G. Ross, Jr.

consumption. The IC also eliminates the recuperator in the PFL, and, unlike the LHP and CPL, the resulting cryogenic system can be tested in any orientation relative to gravity. For space applications, the latter feature will greatly simplify ground testing and qualification prior to launch. It also allows a substantial pressure drop to be incurred across a flow control valve, which raises the possibility of implementing advanced temperature control schemes during periods of system upset[5].

MODEL DEVELOPMENT

Because the gas in the flow loop is supercritical, its temperature will rise as it absorbs heat from the load. The magnitude of that rise is dependent on the size of the load, the specific heat of the gas, and the mass flow rate in the loop. In order to design an IC for a specific application (i.e., specified heat load and load temperature) it is necessary to design for a specific mass flow rate. In particular, because buffer volume influences mass flow rate, overall system mass and parasitic heat leak, it is desirable to optimize the volume, keeping it as small as possible while still allowing for the requisite mass flow rate. In this paper we describe an electrical analogue model of the IC and use it to calculate flow rate as a function of loop resistance with buffer volume as a parameter. We assume that the temperature rise around the loop is much smaller than the average loop temperature, so that fluid properties are evaluated at the average loop temperature (taken to be the desired load temperature). We further assume that the flow through the loop is small compared to the total flow through the PTC cold heat exchanger.

The Integrated Circulator consists of a flow loop (resistive inertance), two buffer volumes (compliances), two check valves (resistances) and a pressure source. In the limit that the wavelength of sound is long compared to the characteristic dimension of each component, the IC can be represented by the analogous electrical network shown in Fig. 1, where the acoustic impedances of Inertance, Compliance and Resistance have been represented by the analogous electrical impedances of Inductance (L), Capacitance (C) and Resistance (R), respectively[6]. The check valves are represented by a standard piecewise linear diode characteristic – a forward resistance, a reverse resistance and a threshold voltage that is taken to be zero. Because the systems are analogous, the well known methods of electrical circuit analysis are used to solve for the time dependent flow rates, which are obtained by substituting the appropriate source pressure and acoustic impedances into the solutions. The source pressure is the pressure in the cold heat exchanger of the cryocooler and is given by

$$p_s(t) = P_0 + p_1 \sin(\omega t + \phi), \tag{1}$$

where P_0 is the mean pressure and p_1 is pressure amplitude. The acoustic impedances are described in Table 1.

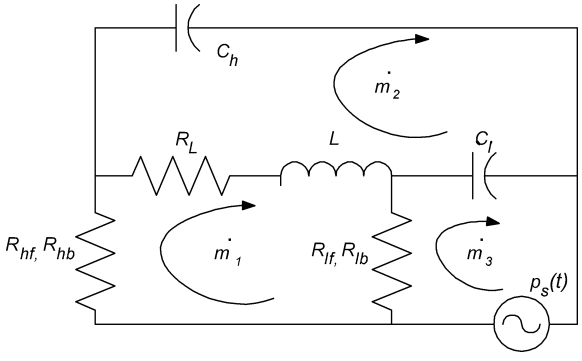

Figure 1. Integrated Circulator – schematic of lumped component representation using electrical analogy

Table 1. List of IC components, acoustic impedance type, symbol and definition in terms of geometry and operating parameters

Component	*Impedance Type*	*Symbol* [(1)]	*Definition* [(2)]	*Units*
High pressure check valve	Resistance	R_{hf}, R_{hb}	$P/\dot{m}$	$m^{-1}s^{-1}$
Low pressure check valve	Resistance	R_{lf}, R_{lb}	$P/\dot{m}$	$m^{-1}s^{-1}$
High pressure buffer volume	Compliance	C_h	V/a^2	$m \cdot s^2$
Low pressure buffer volume	Compliance	C_l	V/a^2	$m \cdot s^2$
Flow loop	Resistance	R_L [(3)]	$P/\dot{m}$	$m^{-1}s^{-1}$
Flow Loop	Inertance	L	ℓ/A	m^{-1}
Pressure source	NA	P_s	Pulse tube pressure	Pa

(1) R_f = forward resistance, R_b = backward resistance
(2) P = pressure (Pa), $\dot{m}$ = mass flow rate (kg/s), M = molecular weight of refrigerant gas (kg/mol), a = speed of sound (m/s), A = cross sectional area of flow loop based on i.d. (m^2), ℓ = flow loop length (m)
(3) R_L is the sum of the hydrodynamic resistance to flow through the loop plus that through any control valve that may be included in the loop.

Use of the piecewise linear diode characteristic has specific implications for the model. Fig. 2 shows typical steady-state pressures in the cold heat exchanger and high and low buffers as functions of time, for the nth cycle. Here, steady state refers to the condition that successive cycles repeat exactly. We define the following times ($t_{m,n}$) for the nth cycle: $t_{1,n}$ = time at which high pressure check valve opens, $t_{2,n}$ = time at which high pressure check valve closes, $t_{3,n}$ = time at which low pressure check valve opens, $t_{4,n}$ = time at which low pressure check valve closes. Each time is defined relative to the source pressure (i.e., the pressure wave in the cold heat exchanger of the cryocooler) such that it is given by Eq. (1) with $\phi = 0$ when $t = t_0 = 0$. The four times $t_{m,n}$ together with the time $t_{1,n+1} = t_{1,n+T}$, where T is the period of the source pressure, define the nth cycle and divide it into four segments. The source-pressure phase angle, check valve state and check valve resistances for each segment are summarized in Table 2.

We begin by assigning a mass flow rate ($\dot{m}$) to each of the three network meshes in Fig. 1. This leads to three integral-differential equations, based on Kirkoff's Voltage Law, the defining equations for L and C and knowledge of the time dependent source pressure $p_s(t)$.

$$R_h\dot{m}_1 + R_L(\dot{m}_1 - \dot{m}_2) + L\frac{d(\dot{m}_1 - \dot{m}_2)}{dt} + R_l(\dot{m}_1 - \dot{m}_3) = 0 \qquad (2)$$

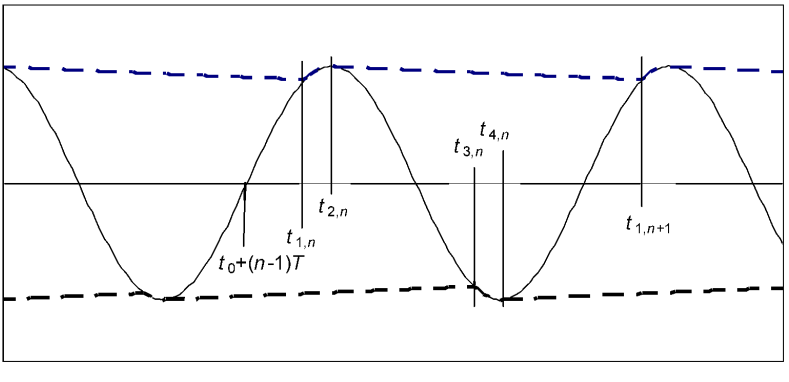

Figure 2. Steady state pressures as function of time for the nth cycle. The solid line is the source pressure; dotted lines are the pressures in the buffers. The times $t_{m,n}$ indicate opening and closing of the check valves.

Table 2. The source-pressure phase angle, check valve state and check valve resistances associated with each time segment of the nth cycle.

Time Segment	*Phase Angle ϕ*	*Check Valve State*	*Check Valve Resistances*
$t_{1,n} \le t < t_{2,n}$	$\omega(t_{1,n} - t_0)$	high pressure open	R_{hf} , R_{lb}
$t_{2,n} \le t < t_{3,n}$	$\omega(t_{2,n} - t_0)$	both closed	R_{hb} , R_{lb}
$t_{3,n} \le t < t_{4,n}$	$\omega(t_{3,n} - t_0)$	low pressure open	R_{hb} , R_{lf}
$t_{4,n} \le t < t_{1,n+1}$	$\omega(t_{4,n} - t_0)$	both closed	R_{hb} , R_{lb}

$$\frac{1}{C_h}\int_{-\infty}^{t} \dot{m}_2\,dt + \frac{1}{C_l}\int_{-\infty}^{t} (\dot{m}_2 - \dot{m}_3)\,dt + L\frac{d(\dot{m}_2 - \dot{m}_1)}{dt} + R_L(\dot{m}_2 - \dot{m}_1) = 0 \tag{3}$$

$$R_l(\dot{m}_3 - \dot{m}_1) + \frac{1}{C_l}\int_{-\infty}^{t} (\dot{m}_3 - \dot{m}_2)dt - p_s(t) \tag{4}$$

Equations (2) through (4) are three independent equations in the three unknown flow rates $\dot{m}_1, \dot{m}_2$ *and* $\dot{m}_3$. To solve them, we first transform them to algebraic equations using Laplace transforms, solve for the transformed variables M_1, M_2 and M_3, then transform back to the time domain to obtain the time dependent flow rates $\dot{m}_1, \dot{m}_2$ *and* $\dot{m}_3$. Finally, we solve for the time dependent component flow rates and pressures of interest.

Taking the Laplace transforms and rearranging leads to the transformed equations L1, L2, L3 and L4

$$P_s(t) = \frac{P_0}{s} + \frac{p_1\left(s\sin(\phi) + \omega\cos(\phi)\right)}{\left(s^2 + \omega^2\right)} \tag{L1}$$

$$(R_h + R_L + R_l + sL)M_1 - (R_L + sL)M_2 - R_l M_3 = L(\dot{m}_1(0) - \dot{m}_2(0)) \tag{L2}$$

$$-(sL + R_L)M_1 + \left(\frac{1}{sC_h} + \frac{1}{sC_l} + sL + R_L\right)M_2 - \frac{M_3}{sC_l} = \frac{p_l(0)}{s} - \frac{p_h(0)}{s} - L(\dot{m}_1(0) - \dot{m}_2(0)) \tag{L3}$$

$$-R_l M_1 - \frac{M_2}{sC_l} + \left(R_b + \frac{1}{sC_l}\right)M_3 = P_s(t) - \frac{p_l(0)}{s} \tag{L4}$$

Where $P_s(t)$ is the transform of the source pressure and the values at t = 0 are the appropriate initial conditions.

With knowledge of the source pressure, the equations L2 through L4 are readily solved for the transformed flow rates M_1, M_2 and M_3 by use of Cramers Rule, which we have implemented in EES[7], and transformed back to the time domain using the method of partial fractions.

Equations L2 through L4 are solved separately for the *m* time segments in each of *n* cycles. Initial conditions for the first segment of the first cycle are taken to be no flow in the loop with both buffers at the mean pressure and a phase angle of zero. The initial conditions and phase angle are subsequently updated for each successive value of *m* and *n*. The value of *n* is chosen such that the values of $t_{m,n}$ for $n>i$, remain constant from cycle to cycle. For reasonably small buffers this happens in less than 20 cycles. In general, then, we set n = 20.

Solutions for the case that the loop is over-damped have the form

$$\dot{m}_{j,m,n}(t) = A_{j,m,n}e^{-\alpha_m t} + B_{j,m,n}e^{-\beta_m t} + C_{j,m,n}e^{-\gamma_m t} + D_{j,m,n}\sin(\omega t + \phi_{m,n}) + E_{j,m,n}\cos(\omega t + \phi_{m,n}) \tag{5}$$

and for the case that the loop is under-damped

$$\dot{m}_{j,m,n}(t) = A_{j,m,n}e^{-\alpha_m t} + e^{-\beta_m t}\left(B_{j,m,n}\sin(\gamma_m t) + C_{j,m,n}\cos(\gamma_m t)\right) + D_{j,m,n}\sin(\omega t + \phi_{m,n}) + E_{j,m,n}\cos(\omega t + \phi_{m,n}) \tag{6}$$

The critically damped solution is not considered because, when doing parametric studies of system behavior, the probability of picking a combination of component values for which the

damping coefficient and natural frequency are exactly the same (the requirement for critical damping) is extremely small.

MODEL VERIFICATION

By careful choice of specific resistances and compliances, the circuit used to approximate the IC can be made to closely resemble a number of circuits that lend themselves to simple analysis and hand calculations. We used this method to verify IC model calculations. Two such cases are described below.

Case 1. Set $R_{hf} = R_{hb} = R_{lf} = R_{lb} >> R_L$. These values result in the IC approximating a source-free series RLC circuit, as shown in Fig. 3, where the compliance C is given by the series combination of C_l and C_h. The initial conditions are taken to be an initial current of zero and an initial pressure in the high pressure buffer of 1.2×10^5 Pa. A plot of mass flow rate versus time for this case is also shown in Fig. 3. The discreet points are from the hand calculation while the solid line represents the result obtained using the IC model with the check valve resistances set to 1×10^{40} $m^{-1}s^{-1}$.

Case 2. Set the high pressure check valve resistances and high pressure buffer volume to zero ($R_{hf} = R_{hb=} C_h = 0$) and the low pressure check valve resistances to values much greater than the loop resistance ($R_{lf} = R_{lb} >> R_L$). In this limit, the IC approximates the forced series RLC circuit pictured on the left in Fig. 4. Initial conditions are taken to be an initial current of zero and an initial pressure in the buffer equal to P_0. A plot of mass flow rate versus time for this case is shown on the right in Fig. 4. In both cases, there is excellent agreement between the IC model and the hand calculations.

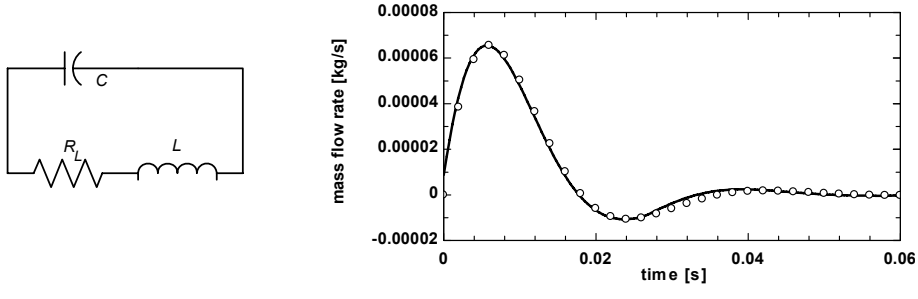

Figure 3. (Left) Series RLC circuit that is approximated when the check valve resistances approach infinity. In practice this means they are much greater than the loop resistance. (Right) Plot of flow rate (kg/s) versus time comparing hand calculation and IC model calculation, for the underdamped case.

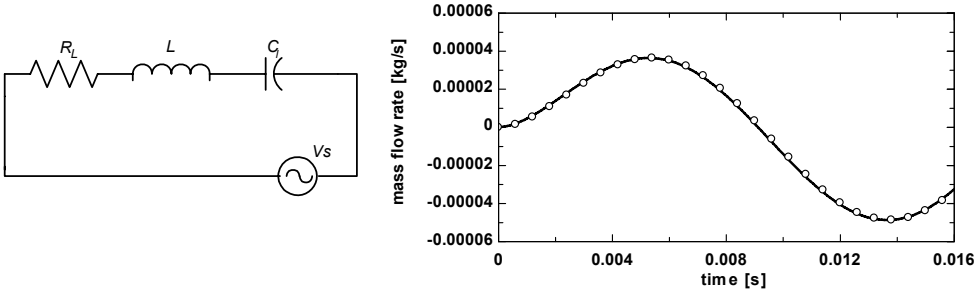

Figure 4. (Left) Forced series RLC circuit that is approximated when the high pressure check valve resistances and C_h are zeroed and the low pressure check valve resistances approach infinity. (Right) Plot of flow rate (kg/s) versus time comparing hand calculation and IC model calculation for the overdamped case.

COMPARISON OF MODEL CALCULATIONS WITH EXPERIMENTAL RESULTS

In order to validate the IC model against actual data, we measured the mass flow rate in the cooling loop of an IC attached to a pulse tube cooler, for two different buffer volumes. We included a metering valve in the loop to control the flow rate and accounted for it in the IC model by adding its resistance to that of the flow loop tubing. The metering valve is instrumented with two Endevco pressure sensors located outside the vacuum space at the end of capillary sense lines. The sense lines were calibrated at room temperature by installing them on the high and low pressure buffers of the IC, with the check valves removed, and instrumenting the arrangement with a set of pressure sensors directly on the buffers and a second set on the sense lines. The pressure amplitude was varied by varying the stroke of the pulse tube pressure wave generator. This calibration together with the manufacturer's values of C_v for the valve, as a function of turns open, gives a measure of the mass flow rate for any known setting of the valve. Other details of the test setup are described elsewhere[8].

Measured mass flow rates are compared to calculated flow rates in Fig. 5, as a function of turns open, for two buffer sizes: 1.5 cc and 13.4 cc. The open symbols are data from the larger buffers, while the solid symbols are data from the smaller buffers. The solid lines represent the results of calculations from the IC model using check valve resistances measured in a D.C. flow test apparatus (both forward and reverse). Buffer volume compliances and flow loop inertance and resistance are all determined from their dimensions according to the expressions listed in Table 1. The metering valve resistance is determined for a given number of turns open from the manufacturer's published values of C_v. While it is not evident in Fig. 5, it was necessary to include the volume of the flow loop, including estimates of the internal volumes of the metering valve and a number of VCR fittings. When this additional volume is included, the agreement seen in Fig. 5 is obtained. Note that the model captures the dependence on flow loop resistance (metering valve turns open) as well as buffer volume. The error bars in the figure represent ±10% of the measured values.

The check valve on the low pressure side of the IC developed some leakage flow during testing of the smaller buffers. We estimated this flow rate from pressure traces and modified the resistance R_{lb} in the IC model accordingly. The agreement between model and data seen in Fig. 5, for the smaller buffers, reflects this adjustment.

As it turns out, all the data shown in Fig. 5 correspond to an over-damped condition. For the pulse tube cooler used in these tests, the average flow rate through the cold heat exchanger is about 4 g/s, so that the maximum average loop flow was approximately 5% of total flow. In future testing we hope to investigate under-damping, as well, and its effects on the average flow rate in the loop. One question to be answered is can an under-damped condition be obtained while maintaining the restriction that loop flow be small relative to flow through the cold heat exchanger.

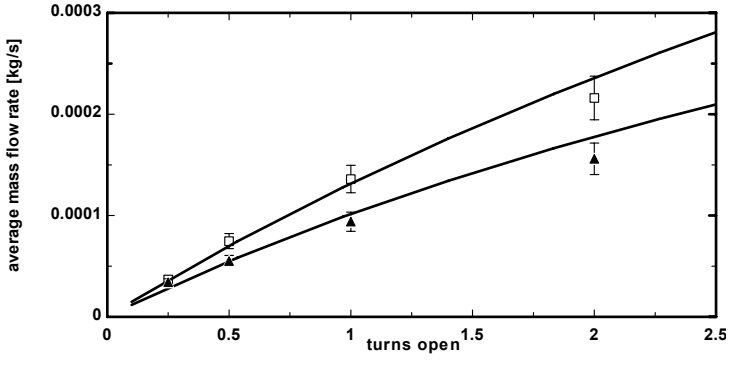

Figure 5. Comparison of modeling results with measured data for two buffer volumes. Solid symbols are for volumes of 1.5 cc, open symbols are for volumes of 13.4 cc each.

Finally, with the small buffers installed no heat was added to the loop; with the large buffers installed 1 watt was added at a heater midway between buffers. The parasitic heat load on the loop is estimated at 2.7 watts while the parasitic load on the buffers is estimated at 2 watts for the larger buffers and 0 watts for the smaller buffers. In all cases, except for the two lowest flow rates with heating, the temperature rise around the cooling loop was small compared to the average temperature. Average loop temperatures ranged from 70 K to 110 K, while temperature rises were less than 7% of the average loop temperature (less than 20% for the lowest flow rates with heating).

SUMMARY

We developed an acoustic model of the Integrated Circulator for regenerative cryocoolers, implemented it in the EES software and used it to calculate the mass flow rate in a cooling loop, with control valve, for two different buffer volumes. To validate the model, we measured the flow rate in a real IC attached to a pulse tube cooler and compared the results to our calculations. It was found that the volume in the flow loop must be included in the model calculations to obtain good agreement between model and data, and it is also important to include the proper reverse resistance for the check valves.

ACKNOWLEDGEMENTS

This work was supported by the Missile Defense Agency through the Air Force Research Laboratory under contract # W9113M-10-P-0057.

REFERENCES

1. Rich, M., Stoyanof, M., and Glaister, D., "Trade studies on IR gimbaled optics cooling technologies," *IEEE Aerospace Applications Conference*, Vol. 5 (1998), pp. 255-267.
2. Hoang, T.T., O'Connell, T.A., Ku, J., Ku, J., Butler, C.D., and Swanson, T.D., "Large Area Cooling for Far Infrared Telescopes," Proceedings *of SPIE, Cryogenic Optical Systems and Instruments X*, Vol. 5172 (2003).
3. Hedayat, A., Hastings, L.J., Bryant, C., and Plachta, D.W., "Large Scale Demonstration of Liquid Hydrogen Storage with Zero Boil-off," *Adv. in Cryogenic Engineering*, Vol. 47B, Amer. Institute of Physics, Melville, NY (2002), p. 1276.
4. Michaelian, M., Nguyen, T., Petach, M., and Raab, J., "Remote cooling with the HEC cooler," *Cryocoolers 15*, ICC Press, Boulder, CO (2009), pp. 541-544.
5. Skye, H.M., Hoch, D.W., Nellis, G.F., Maddocks, J.R., Klein, S.A., Roberts, T. and. Davis, T, "Rectified continuous flow loop for the thermal management of large structures," *Adv. in Cryogenic Engineering*, Vol. 51, Amer. Institute of Physics, Melville, NY (2006), pp.1809-1816.
6. Kinsler, L.E., and Frey, A.R., *Fundamentals of Acoustics, 2nd ed*., John Wiley and Sons, Inc., New York (1962).
7. Klein, S.A., *EES – Engineering Equation Solver, Academic Professional v8.551*, F-Chart Software, www.fchart.com, (2010)
8. Maddocks, J.R., Maddocks, P., Fay, M., Helvensteijn, B.P.M., and Kashani, A., "Performance Test of Pulse Tube Cooler with Integrated Circulator," *Cryocoolers 16*, ICC Press, Boulder, CO (2011), pp. 591-599.